# A metamodel-based multicriteria shape optimization process for an aerosol can

Aalae Benki, Abderrahmane Habbal, Gaël Mathis

Available online at www.sciencedirect.com

ScienceDirect

ELSEVIER

00 (2017) 1–15

# A metamodel-based multicriteria shape optimization process for an aerosol can

Benki Aalae*[a], Habbal Abderrahmane[b], Mathis Gael[c]

[a]*INRIA Sophia Antipolis, OPALE Project Team, 2004 Route des Lucioles, 06902 Sophia Antipolis, France.*
[b]*University Nice Sophia Antipolis, Mathematics Dept, 28 Avenue de Valrose, 06103 Nice Cedex 2, France.*
[c]*ArcelorMittal Global R&D, route de St. Leu 60761 Montataire Cedex France.*

**Abstract**

In this paper, we study a multicriteria shape design of a highly nonlinear mechanical 2D structure, namely the shape optimization of the aerosol can bottom. In fact, it is made depending on two criteria, the dome growth DG and the dome reversal pressure DRP, that define the resistance of the bottom against the internal pressure. This two criteria are known to be conflicting, therefore, a multicriteria optimization problem is formulated to represent the trade-offs among the design parameters. Due to the expensive time-consuming cost to solve this kind of optimization problems (e.g., capturing the Pareto front), the use of a surrogate model (e.g., metamodel) cheap to evaluate is mandatory. For this reason, we have developed an algorithm which is a coupling between the normalized normal constraint method (NNCM) and the radial basis function metamodel (RBF). The NNCM-RBF coupling was tested for several academic test cases and for our industrial problem and the obtained results clearly show the efficiency of our coupling to solve all the problems treated with a remarkable gain in the computational time.

*Keywords:* Aerosol can, multicriteria shape optimization, Normalized normal constraint method, Radial basis function metamodel.

## 1. Introduction

In the wide range of metallic packaging, the aerosol can is one of the most commonly used. One of the main requirements of specifications asked by the customers is the resistance to internal pressure. In fact, the aerosol cans are filled with fluid at high pressure, for this reason, the structural stability of their bottom is then delicate to maintain. The goal of the canmakers is to look for new profiles of the aerosol can's bottom that resists against the internal pressure of the fluid (Fig. 1).

In the present work, we address the problem of shape optimization of the can's bottom , in order to control the dome growth DG (e.g., displacement of can base) at a proof pressure as well as the dome reversal pressure DRP, a critical pressure at which the aerosol can's bottom looses stability (e.g., initiates buckling). Those two criteria are known to be conflicting, therefore, our aim is to identify the Pareto front of this problem ([1]).

In most cases, the identification of the Pareto front for industrial optimization problems (e.g., all the time are structural problems) is very costly in computing time because we need a large number of evaluations for the criteria to be optimized. To overcome this, the most researchers and industry begin to develop algorithms which consist to coupling the conventional methods to capture the pareto front with metamodels aimed at cheap costs evaluation. There are

Figure 1. the bottom of aerosol can before and after losing stability.

two ways to do this coupling: The first idea is to lead optimization with a dedicated algorithm and use an updated metamodel for a certain number of evaluations until finding the solutions (e.g., strong coupling). The second idea is to lead optimization with the metamodel and only do the exact calculations of the obtained solutions (e.g., weak coupling). There are several descriptions of the coupling techniques, see for example ([2],[3],[4] and [5]). In this context, we can cite as examples, some research with different applications as the automotive structures ([6],[7],[8] and [9]), aerodynamic design ([10],[11] and [12]) and the building energy ([13]).

For our work, we have used one of the known methods adapted to the approximation of pareto front which is the NNCM Method ([14],[15] and [16]) coupled a weak coupling to the RBF metamodel ([17],[18] and [19]). Firstly, we have studied the consistency of the NNCM-RBF coupling by solving several standard mathematical benchmarks, then, the coupling is applied to our industrial case, namely the shape optimization of the can's bottom.

The structure of this paper is as follows: Section (2) summarizes the methods used to developed our algorithm with a validation for some academic test cases and Section (3) demonstrates the industrial case with the obtained results. Conclusions and future contributions are listed in Section (5).

## 2. NNCM coupled with the RBF metamodel

This section presents the coupling of NNCM method and the RBF metamodel and its validation through several test cases.

### *2.1. NNCM*

The normalized normal constraint method is an approach proposed by messac and Yehya for generating a set of evenly spaced solutions on a Pareto frontier - for multicriteria optimization problems - ([14]).
Throughout our work, we address a special case of multicriteria optimization problems (two objective functions), we define the mathematical representation of this optimization problem as follows:

$$(P)$$

$$\begin{cases} \min\limits_{x} F(x) = (f_1(x), f_2(x)) \\ subject\ to \begin{cases} x \in (C) \end{cases} \end{cases} \tag{1}$$

In this formulation, the set $(C)$ contain all three types of constraints (equality,inequality and an upper and a lower

bound constraints). The points $x$ that fulfil all the constraints are feasible, while all other points are unfeasible.
For the NNCM method, the optimization takes place in the normalized objective space, the main steps of the method can be summarized in the following points:

Let $x_i^*$ the respective global minimizers of $f_i(x)$ i=1,2 , over $x \in (C)$.

The Utopia and Nadir points are hypothetical points defined respectively by the best and the worst values for each the criteria in the set (Fig. 2). They are written mathematically by the two following formulas $f^U = [f_1(x_1^*), f_2(x_2^*)]$ and $f^N = [f_1(x_2^*), f_2(x_1^*)]$ respectively.
The distances $L_1$ and $L_2$, lying between the two global minimizer points and the Utopia point, are the elements of the following matrix:

$$L = f^N - f^U \tag{2}$$

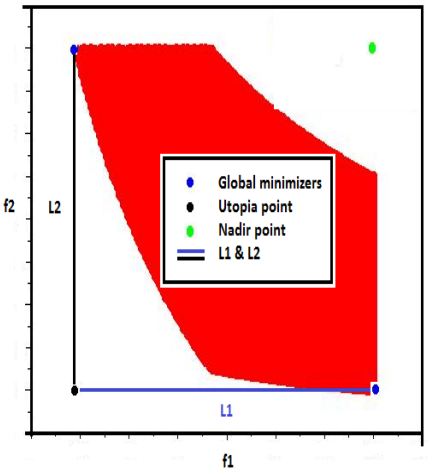


Figure 2. Illustration of the Utopia point, Nadir points, and The L1 and L2 distances required by the NNCM method.

Using the above definitions, the normalized objective space $\overline{F}$ can be evaluated as:

$$\overline{F}(x) = (\overline{f}_1(x) = \frac{f_1(x) - f_1(x_1^*)}{L_1} \quad , \quad \overline{f}_2(x) = \frac{f_2(x) - f_2(x_2^*)}{L_2}) \tag{3}$$

Let define $\overline{N}_1$ as the direction from $x_1^*$ to $x_2^*$ which is called Utopia line:

$$\overline{N}_1 = \overline{F}_2^* - \overline{F}_1^* \tag{4}$$

where $\overline{F}_i^* = [\overline{f}_1(X_i^*), \overline{f}_2(X_i^*)]$

We generate a set of evenly distributed points on the Utopia line as:

$$\overline{X}_{pk} = \sum_{k=1}^{2} \beta_{pk} \overline{F}_k^* \tag{5}$$

where $\sum_{k=1}^{2} \beta_{pk} = 1 \quad ; \quad 0 \leq \beta_{pk} \leq 1$

Using the set of evenly distributed points on the Utopia line, we generate a corresponding set of Pareto points by solving a succession of optimization runs of the $P_{NNCM}$ problem defined in (Eq.6). Each optimization run corresponds to a point on the Utopia line (Fig. 3).

$$(P_{NNCM})$$

$$\begin{cases} \min\limits_{x} \ \overline{f}_2(x) \\ subject\ to \begin{cases} \overline{N}_1(\overline{F}-\overline{X}_{pk})^T \leq 0 \\ x \in (C) \end{cases} \end{cases} \tag{6}$$

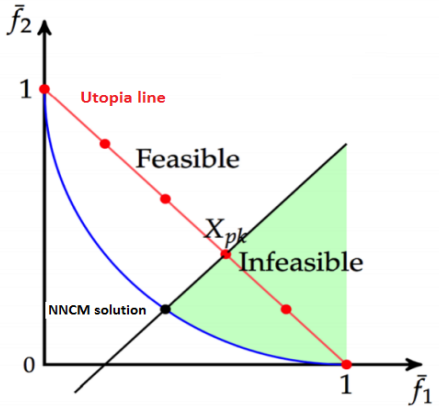


Figure 3. Graphical representation of the normalized normal constraint method for bi-objective (two criteria) problem

### 2.2. RBF

Radial basis functions (RBF) have been developed for scattered multivariate data interpolation ([19]). The method uses linear combinations of a radially symmetric function based on Euclidean distance or other such metric to approximate response functions. There exist many different kinds of radial basis function, Schaback presents in his paper ([20]) a full Comparison of radial basis function interpolants. We conclude from this study that the simple classical form (Eq. 7) remains the best and the most formula used by the majority of researchers:

$$\tilde{f}(x) = \sum_{i=0}^{n} \omega_i \phi(||x - x_i||) \tag{7}$$

where n is the number of sampling points, x is the vector of design variables, $x_i$ is the vector of the $i^{th}$ sampling point, $||x - x_i||$ is the Euclidean distance (e.g., The norm is usually Euclidean distance, although other distance functions are also possible.), $\phi$ is a basis function (for example, Gaussien one $\phi(r) = e^{-a_f r^2}$ where $a_f$ is the attenuation coefficient $(0 \prec a_f \leq 1)$), and $\omega_i$ is the unknown weighting coefficient which is obtained by solving the linear system:

$$\mathbf{f} = \mathbf{A}.\omega \tag{8}$$

where $\mathbf{f} = [f(x_1), .., f(x_n)]^T$ and $\mathbf{A}_{i,j} = \phi(||x_i - x_j||)$ $(i = 1, .., n; j = 1, .., n)$.

The RBF metamodel formula (Eq. 7) can be written as:

$$\tilde{f}(x) = \sum_{i=0}^{n} \omega_i e^{-a_f ||x - x_i||^2} \tag{9}$$

To have a good metamodel at the level of precision, we must make a judicious choice for choosing the sampling points $x_i$ and the attenuation factor's value $a_f$. The choice of these elements influences directly the results.

### 2.3. *Effect of the attenuation factor*

The attenuation factor in radial basis function has a critical influence on the accuracy of the interpolation model. We illustrate this with a numerical example. The RBF metamodel is constructed for the quadratic-sine function (Eq. 10) using the same sampling points data -10 equally spaced points in [0,2]- (Fig. 4).

$$f(x) = x(1-x)sin(2\pi x), \quad x \in [0,2] \tag{10}$$

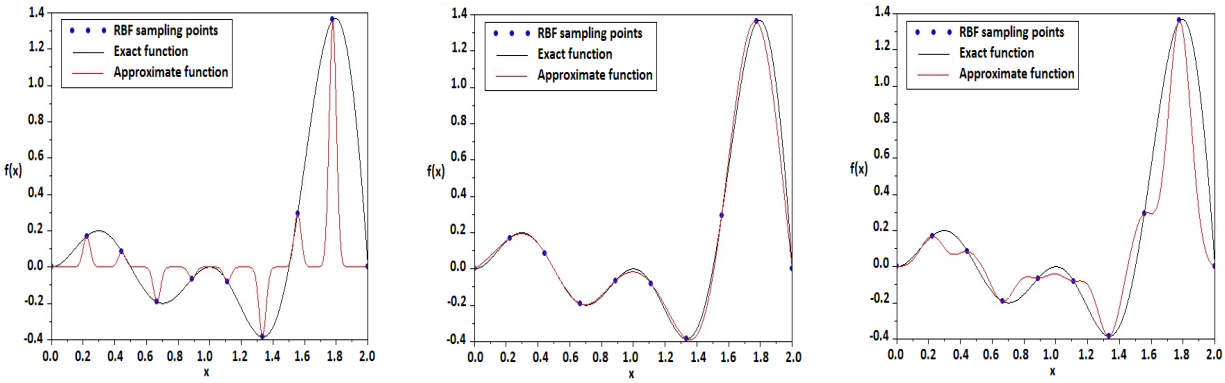


$a_f$=0.1 $a_f$=0.5 $a_f$=0.9

Figure 4. Illustration of the influence of the attenuation factor's value chosen for the RBF calculation of the approximate function (red) for the quadratic-sine function (black) keeping the same sampling points (blue points) for the construction of the metamodel.

In his paper ([23]), Rippa discussed several empirical methods for choosing the best attenuation factor and he presents his technique called "rippa technique" to search the optimized value of this factor based on the leave-one-out validation ([21]).

**Algorithm 1** leave-one-out validation - LOOV

1: **Input**: $N$ the total number of RBF sampling points $x_i$ and $a_0$ the initial attenuation factor
2: **For** $n = 1 : N$
3: $x^{(n)} = \{x_1, x_2, ..., x_{n-1}, x_{n+1}, ...x_N\}$ ▷
4: $\tilde{f}^{(n)}(x,a) = \sum_{m=1, m\neq n}^{N} \omega_m^{(n)} \phi(||x - x_m||)$
5: $E_n = f(x_n) - \tilde{f}^{(n)}(x_n, a) = \frac{\omega_n}{\mathbf{A}^{-1}_{n,n}}$ ▷
6: **End For**
7: $E(a) = [E_1, E_2, ..., E_N]^T$
8: $a_f = \underset{a}{\text{argmin}} ||E(a)||$
9: **Output**: The optimized attenuation factor $a_f$

The computation of $E(a)$ requires the solution of $N$ linear equations of order $(N-1)*(N-1)$, the total number of operations is of order $N^4$ which can be very expensive. An efficient algorithm is given by Rippa requires only one LU decomposition to compute the $E(a)$, he demonstrated that:

$$E_n = \frac{\omega_n}{\mathbf{A}^{-1}{}_{n,n}}, \quad n = 1 : N \tag{11}$$

where $\omega_n$ is the $n^{th}$ element of the solution vector $\omega$ and $\mathbf{A}^{-1}$is the invertible matrix of $\mathbf{A}$ defined in the (Eq. 8).

### 2.4. *Effect of the sampling points*

To show this effect, we use the RBF metamodel to approximate the quadratic-sine function with different database of sampling points (e.g. database generated by three different methods (Fig. 5) and from the obtained results which are presented in the figure (Fig. 6), we can conclude that the uniform distribution gives us the best approximation.

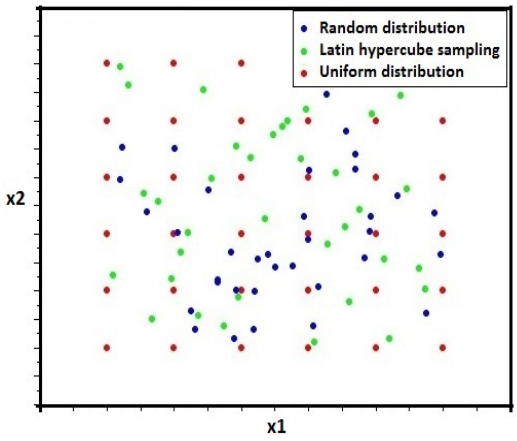


Figure 5. Example of sampling points generated by different methods: Random distribution (blue points), Latin hypercube sampling (green points) and the Uniform distribution (red points) for a 2D problem.

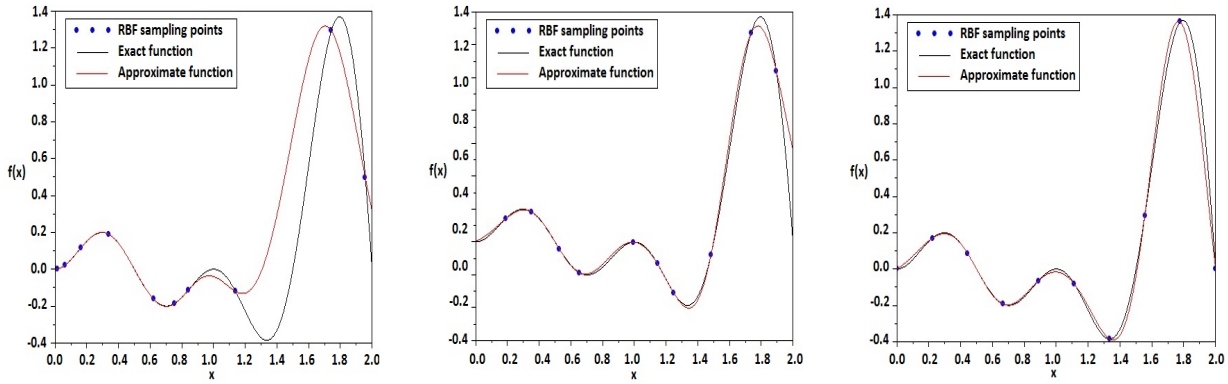


(a) Random distribution (b) Latin hypercube sampling (c) Uniform distribution

Figure 6. Illustration of the influence of the choice of the sampling points generated by several methods (a, b and c) for the RBF calculation of the approximate function (red) for the quadratic-sine function (black) .

This example is one of a full comparative study with several function tests presented in my thesis ([22]). This study led us to choose the uniform distribution as a method to generate the sampling points in order to construct the RBF metamodel.

### *2.5. The NNCM RBF coupling*

Our aim is to couple the NNCM method and RBF metamodel in order to have a simple algorithm with a reasonable and reduced calculation time to solve multicriteria optimization problems. The NNCM-RBF coupling is presented in detail (see algorithm 2) and tested for several optimization problems known as test problems, which are mathematical explicit functions (Hab3d, Fonseca and Tanaka problem).

**Algorithm 2** The NNCM-RBF algorithm

1: **Input**: Let $(P)$ the problem to be solved, $N$ the total number of RBF sampling points and $a_0$ the initial attenuation factor

$$\begin{cases} \min\limits_{x} F(x) = (f_1(x), f_2(x)) \\ subject\ to \begin{cases} x \in (C) \end{cases} \end{cases}$$

2: $x^{(N)} = \{x_1, x_2, , ...x_N\}$ ▷ Uniform RBF sampling points

3: $a_f$ = RIPPA $(f_1, f_2, x^{(N)}, a_0)$ ▷ The optimized attenuation factor by Rippa technique

4: $(\tilde{f}_1, \tilde{f}_2)$ = RBF $(f_1, f_2, x^{(N)}, a_f)$ ▷ The approximate functions by RBF metamodel

5: $x_i^* = \min\limits_{x} \tilde{f}_i(x) \qquad \mathrm{i} = 1:2$ ▷ Minimise each function

6: $\tilde{F}^u = [\tilde{f}_1(x_1^*), \tilde{f}_2(x_2^*)]^T$ ▷ Utopia point

7: $\tilde{F}^n = [\tilde{f}_1(x_2^*), \tilde{f}_2(x_1^*)]^T$ ▷ Nadir point

8: $L = \tilde{F}^u - \tilde{F}^n$ ▷ Matrix of distences

9: $\overline{f}_i(x) = \frac{\tilde{f}_i(x) - \tilde{f}_i(x_i^*)}{L_i} \qquad \mathrm{i} = 1:2$ ▷ Normalized functions

10: $\overline{F}_i^* = [\overline{f}_1(x_i^*), \overline{f}_2(x_i^*)]^T \qquad \mathrm{i} = 1:2$

11: $\overline{N}_1 = \overline{F}_2^* - \overline{F}_1^* \qquad \mathrm{i} = 1:2$ ▷ Utopia line

12: $\overline{X}_{kj} = \sum\limits_{k=1}^{2} \beta_k \overline{F}_k^*,\ \beta_i \geq 0\ ,\ \sum\limits_{i=1}^{2} \beta_i = 1$ ▷ generate points on the Utopia line

13: **For** each $\beta = (\beta_1, \beta_2)^T$ **solve** the $(P_{NNCM})$ problem:

$$\begin{cases} \min\limits_{x} \ \overline{f}_2(x) \\ subject\ to \begin{cases} \overline{N}_1 (\overline{F} - \overline{X}_{pk})^T \\ x \in (C) \end{cases} \end{cases}$$

14: **End For**

15: **Output**: NNCM-RBF solutions

The results, (Fig. 7 and Table 1), show that the coupling NNCM-RBF converges to the Pareto frontier with fewer number (69%, 96% and 89%, for Fonseca, Tanaka and Hab3, respectively) of calls for the objective functions compared to a conventional NNCM.

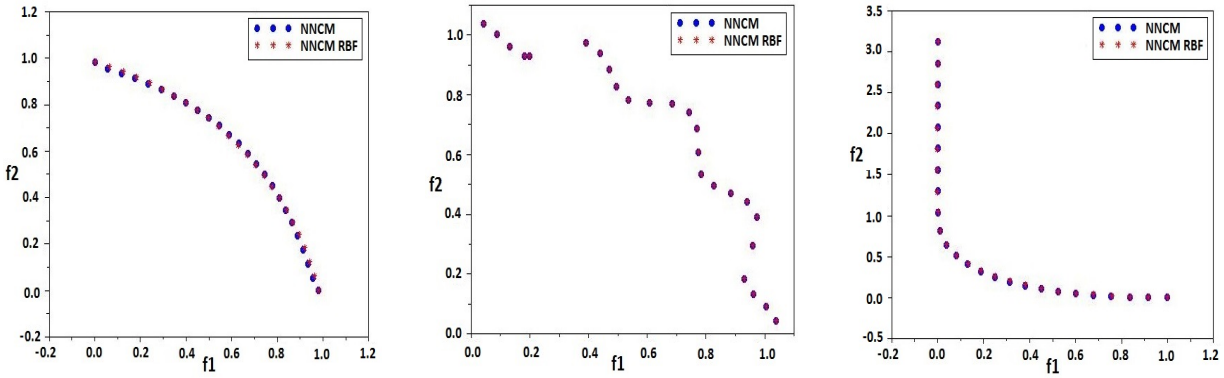


Figure 7. Comparison between the results obtained by NNCM-RBF approach (in red), and the exact solutions NNCM (in blue)

Table 1. Functions call number required by NNCM and NNCM-RBF methods

| Problem | Method used | Prescribed Pareto points (P.N) | Functions calls |
|---|---|---|---|
| Fonseca | NNCM | 25 | 406 |
| | NNCM-RBF | 25 | 128 |
| Tanaka | NNCM | 25 | 886 |
| | NNCM-RBF | 25 | 32 |
| Hab3 | NNCM | 25 | 704 |
| | NNCM-RBF | 25 | 64 |

After the validation of the coupling NNCM-RBF for the academic test cases, the practical case of shape optimization of the bottom of the aerosol can was considered.

## 3. Aerosol can

### *3.1. The aerosol can model*

In the present study a 2D model provided by Arcelor mittal company and developed with ls dyna software was used to predict of the behavior of the aerosol can's bottom when submitted to pressure. In fact, the aerosol can is considered axisymmetric, therefore, only a half generating two dimensional (2D) will be sufficient to represent the entire can. The assumption of 2D calculations are so near from the reality (Fig. 8).

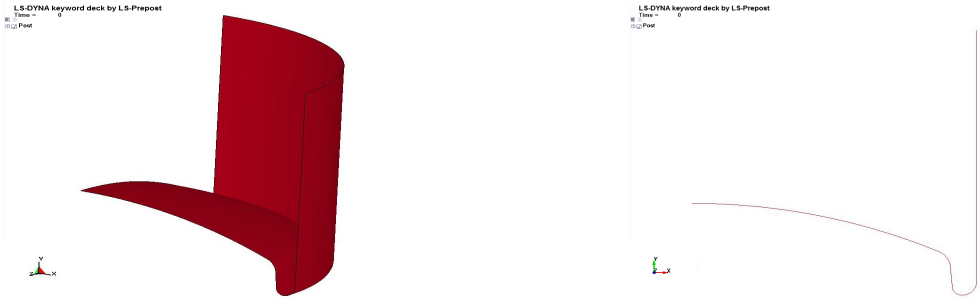


Figure 8. Visualization of the aerosol can - Ls dyna models -: the 3D model (a) and its 2D equivalent model (b)

For our work, we use two types of bottom's cans (Fig. 9), the aerosol cans are made of thin high performance steel which have the characteristics shown in the table 2.

Table 2. Process parameters used in simulation

| Process Parameter | Value or law |
|---|---|
| Thick steel (e) | 0.46 mm |
| Strain hardening exponent (n) | 0.2 |
| Yield strength (Re) | 270 MPa |
| Ultimate strength (Rm) | 380 MPa |
| Strength coefficient | $K = e^{(Rm.(n.(1-ln(n))))}$ |
| Hollomon law | $\sigma = K\varepsilon^n$ |

Aerosol bottom N1 Aerosol bottom N2

Figure 9. The two shapes of the aerosol can's bottom used in our study ( N1 and N2 )

### 3.2. *Calculation of criteria*

During charging, there is pressure acting on the aerosol can's bottom. To extract DRP value, it is necessary to calculate the pressure when the model deforms and it can not resist more than threshold. This time is when the model switch from implicit to explicit calculation $T_{switch}$. For extracting DG value, we need just read the displacement of the point A on the foot of the aerosol can in the moment $T_{switch}$ (Fig. 10).

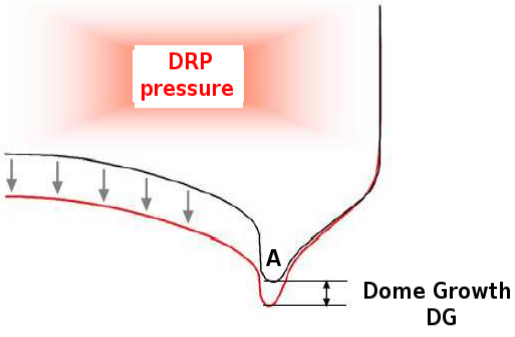


Figure 10. Two criteria to be optimized **DRP** vs **DG**. DRP is the critical pressure where the can bottom loses stability and DG is the calculated displacement of the point A at the time where DRP pressure is detected

The figure (Fig. 11) shows an example on how to extract the criteria to be optimized in our industrial case by the ls dyna software.

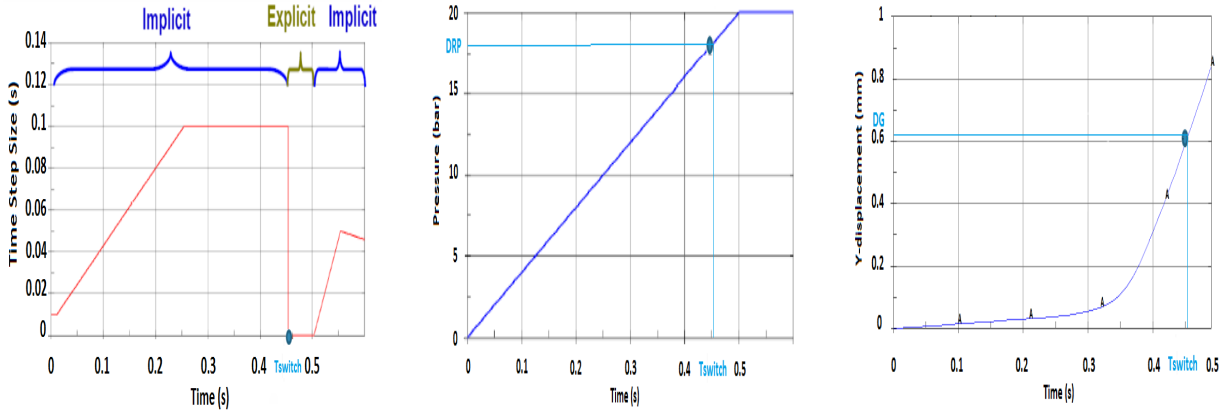


(a) $T_{switch}$ (b) DRP (c) DG

Figure 11. Example of extracting the DRP and DG criteria from Ls dyna: (a) $T_{switch}$ : The time where the can bottom loses stability, (b) DRP is the critical pressure at the time $T_{switch}$ and (c) DG is the calculated displacement of the point A at the time $T_{switch}$

We define the mathematical representation of the two criteria as follows:

$$\begin{cases} DRP{=}Pression(T_{switch}) \\ DG \ {=}Displacement((A)_{T_{switch}}) \end{cases} \tag{12}$$

## 4. Shape optimization process

### *4.1. Shape optimization - problem description -*

The aim is to find an ideal new form of the bottom which satisfies the required bottom's resistance according to the customer's requirement better than the initial shape used which have the values given in the table 3.

Table 3. Intial shapes of the aerosol can used - DRP and DG values-

| Aerosol can | DRP (bar) | DG (mm) |
|---|---|---|
| N1 | 19.1092 | 0.8975 |
| N2 | 15.2 | 0.4749 |

The goal is to figure out a design of the aerosol cans bottom which satisfies a DRP value bigger than DRP of initial shapes and a DG value smaller than 1 mm.

Firstly, 4 points on the initial shape are selected as the design variables. By changing the position of each points (3 positions), a set of 81points is obtained, where each point represents a given shape of the can bottom (Fig. 12). Then, for each point, the exact values of the two criteria DRP and DG are calculated. These values are collected to set a database of the sampling points allowing building the RBF metamodel for each criterion.

The design variables can only moving in one direction - in the vertical direction for $(\varphi_1, \varphi_2, \varphi_3)$ and the horizental one for $(\varphi_1)$ -.

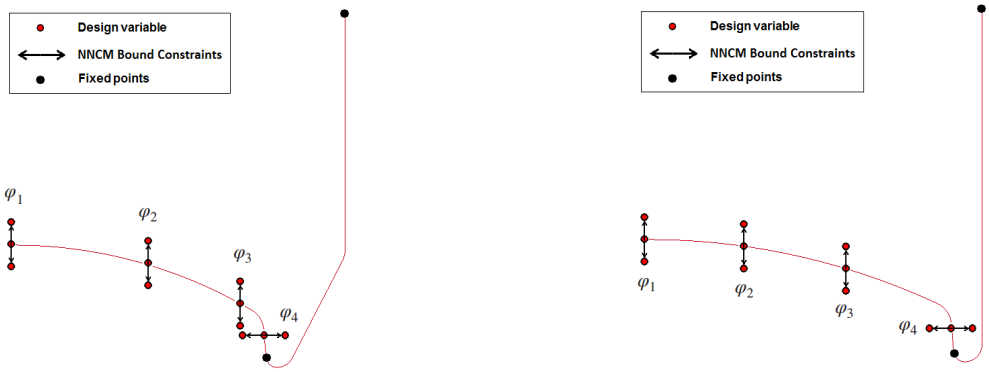


Aerosol bottom N1 Aerosol bottom N2

Figure 12. Four design variables $(\varphi_1, \varphi_2, \varphi_3, \varphi_4)$ and for each point three different positions allowing to have a combination of 81 elements, and each element representing a given shape of the aerosol can's bottom

Let $\varphi_0 = (\varphi_{01}, \varphi_{02}, \varphi_{03}, \varphi_{04})$ the initial shape, and $\alpha$ a positive offset. Then, we choose the bound constraints as follows:

* $\varphi^{lower} = (\varphi_{01} - \alpha, \varphi_{02} - \alpha, \varphi_{03} - \alpha, \varphi_{04} - \alpha)$
* $\varphi^{upper} = (\varphi_{01} + \alpha, \varphi_{02} + \alpha, \varphi_{03} + \alpha, \varphi_{04} + \alpha)$

Finaly, The industriel problem can be as the following formula:

$$\max_{\varphi=(\varphi_1,\varphi_2,\varphi_3,\varphi_4)} DRP(\varphi) \;/\; \min_{\varphi=(\varphi_1,\varphi_2,\varphi_3,\varphi_4)} DG(\varphi)$$
$$subject\ to\ \left\{\ \varphi^{lower} \leq \varphi \leq \varphi^{upper}\right. \tag{13}$$

*4.2. Shape optimization - result and discussion -*

For $\alpha = 0.5mm$, we computed an approximate Pareto front for the DG/DRP costs using our developed algorithm the NNCM-RBF coupling with different prescribed number of Pareto points (P.N=6,12,24). The figures (Fig. 13 and Fig. 14) show the Pareto front obtained for the two study cases by our coupling and their exact evaluation. The table4 and the table5 show the overall time and total number of exact or surrogate evaluations used for the aerosol bottoms N1 and N2 respectively.

Table 4. Time required for the different functions call - Aerosol bottom N1 - (***)=(*)+(**)

| (P.N) | Total *time**** | Objective function | | approximated function | |
|---|---|---|---|---|---|
| | | Call number | Time required** | Call number | Time required* |
| 6 | 3h 50 min 12 s | 87 | 3h 22 min 56 s | 90124 | 25 min 16 s |
| 12 | 4h 13 min 51 s | 93 | 3h 42 min 012 s | 91212 | 31 min 39 s |
| 24 | 4h 35 min 55 s | 105 | 4h 03 min 09 s | 91868 | 32 min 46 s |

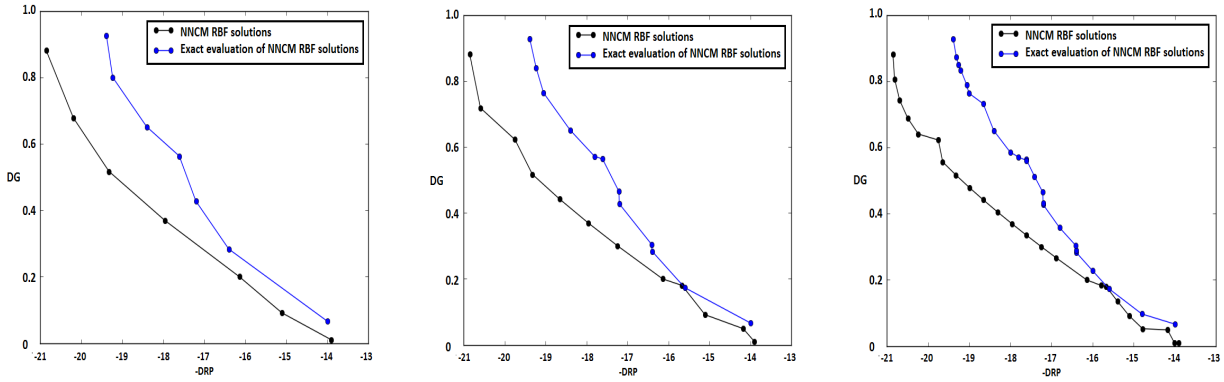


Figure 13. Comparison between the results obtained by NNCM-RBF approach (in blue), and the exact cost evaluation of these results (in red) for several cases - Aerosol bottom N1 -

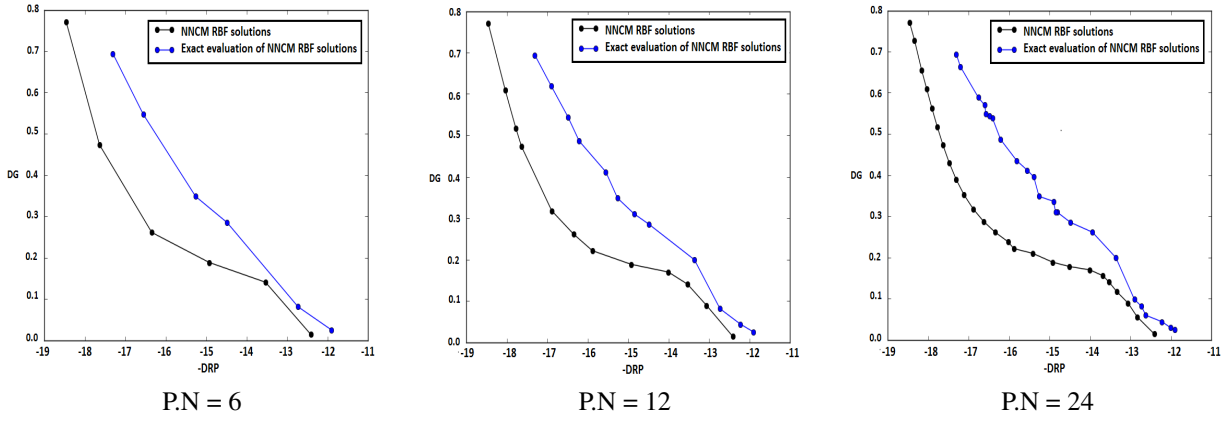


Figure 14. Comparison between the results obtained by NBI RBF approach (in blue), and the exact cost evaluation of these results (in red) for several cases - Aerosol bottom N2 -

Table 5. Time required for the different functions call - Aerosol bottom N2 - (***)=(*)+(**)

| (P.N) | Total *time**** | Objective function | | approximated function | |
|---|---|---|---|---|---|
| | | Call number | Time required** | Call number | Time required* |
| 6 | 4h 26 min 44 s | 87 | 4h 01 min 26 s | 77924 | 25 min 26 s |
| 12 | 4h 44 min 00 s | 93 | 4h 14 min 58 s | 79112 | 29 min 02 s |
| 24 | 5h 28 min 02 s | 105 | 4h 52 min 17 s | 80008 | 35 min 45 s |

We can notice from the tables (4 and 5) that our approach has allowed us to save a remarkable computational time. For example, if we take the case (P.N = 24) from the second case (N2) (Table 5), there are 105 calls of exact function evaluations and 80008 for approximated function, respectively, which represent 0.14 % and 99.86 % of the total function calls used in our approach. But at the same time, we note that only this 0.14% of total calls take 89.10%of the total computing time required. This last remark justifies why we chose not to apply roughly the NNCM method with exact evaluations to solve this industrial case.

A simple comparison between the results obtained by our approach and the accurate evaluation of these solutions (Fig. 13 and Fig. 14) allows us to assess that our results remain good ones notwithstanding the complexity of our cases study.

we remarked also that all solutions are almost located at the boundary of the space formed by the elements of the RBF database (e.g. sampling points) (Fig. 15). Then we can conclude that the solutions obtained are likely NNCM solutions and our approach is able to solve the industrial problem with a reasonable computation time.

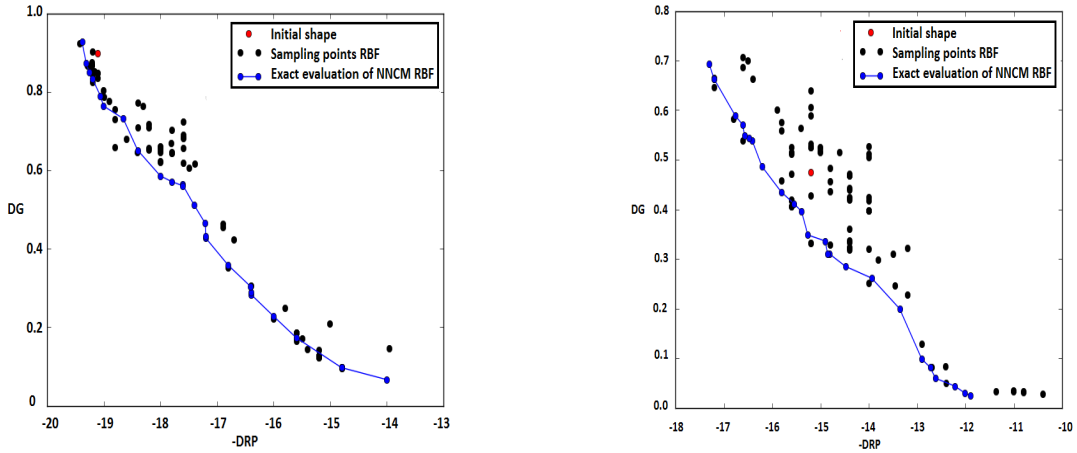


Figure 15. Superposition of the results obtained by our NNCM-RBF approach (in blue), the RBF database (in black) and the initial solution (in red)

Finally, we close this section by presenting the new profiles of the aerosol can that meet industrial requirements (Fig. 16 and Fig. 17).

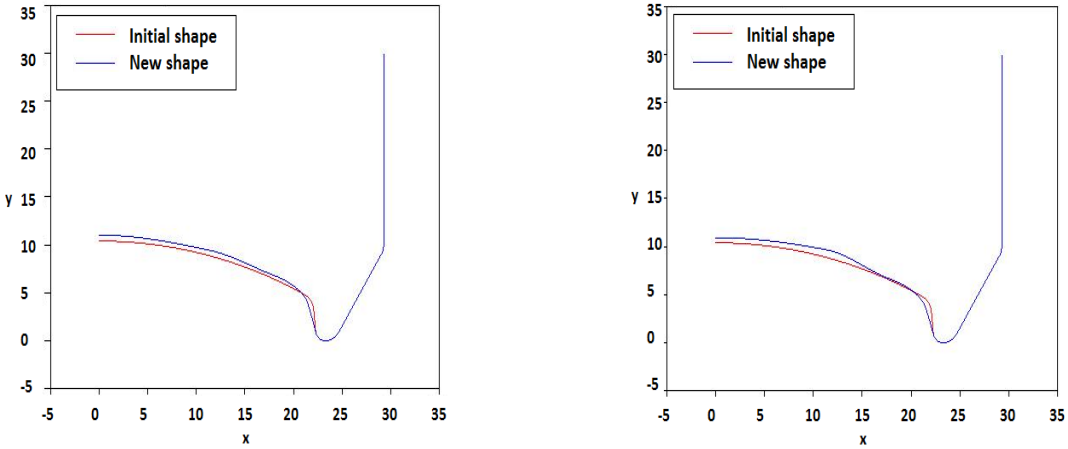


Figure 16. Some new profiles of the aerosol bottom N1 which meet the operational industrial requirements

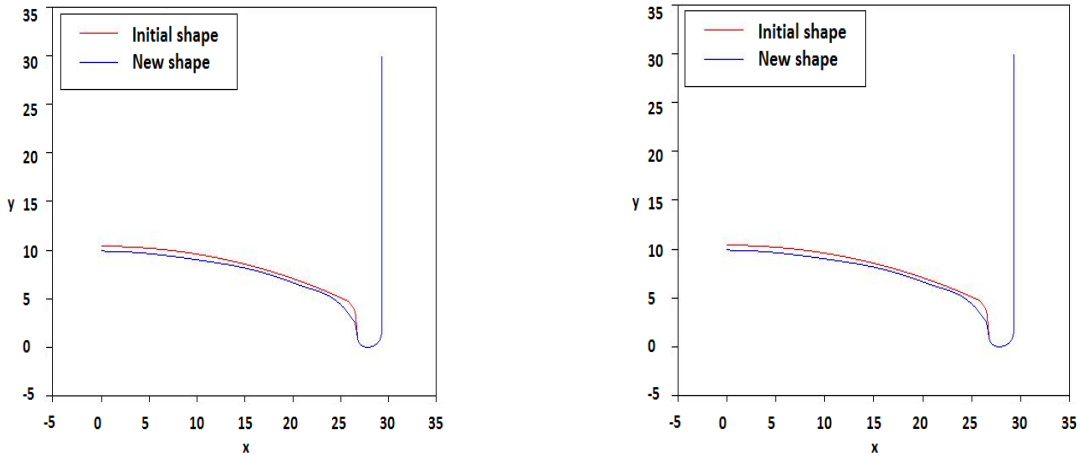


DRP = 15.8084 , DG = 0.4347 DRP = 17.3041 , DG = 0.6938

Figure 17. Some new profiles of the aerosol bottom N2 which meet the operational industrial requirements

## 5. Conclusion

This research proposed an optimization algorithm for solving an industrial multicriteria optimization problem namely the shape optimization of the aerosol can's bottom. The algorithm is a weak coupling between the NNCM method adapted to the capture of the Pareto front and the RBF metamodel used to construct cheap surrogate models of the criteria to be optimized. The coupling is used to avoid the very expensive calculation time due to the cost evaluation of the real criteria.
the appropriateness and effectiveness of the proposed algorithm were verified by several academic cases and the industrial problem, and it also allowed us to identify new profiles of the aerosol can which satisfies the industrial requirements. Although proposed algorithm was applied to the two kinds of the aerosol can's bottom in this paper, other products have similar issues. Therefore, proposed coupling is expected to apply to other cases in the current industry fields.
The future research direction of our work is the study of the 3D model of the aerosol can with a new version of the coupling NNCM-RBF where the RBF metamodel will be updated during the optimization process to make the model more efficient.

## 6. Acknowledgments

The present work was achieved within the framework of the partnership between the research center INRIA Sophia Antipolis and leader company in the steel manufacturer ArcelorMittal France, which funded this work.

## References

[1] Miettinen K.M.; 1999. Nonlinear Multiobjective Optimization. *Kluwer Academic*, Boston, pp 298-299.
[2] Simpson T., Peplinski J., Koch P. N., Allen J.; 2001. Metamodels for computer-based engineering design: survey and recommendations. *Engineering with Computers*, Vol 17, Issue 2, pp 129-150.
[3] Queipo N. V., Haftka R. T., Shyy W., Goel T., Vaidyanathan R., Tucker P. K.; 2005. Surrogate based analysis and optimization. *Progress in Aerospace Sciences*, Vol 41, Issue 1, pp 1-28.
[4] Wang G. G., Shan S. ; 2007. Review of metamodeling techniques in support of engineering design optimization. *Journal of Mechanical Design*, Vol 129, Issue 4, pp 370-380.
[5] Forrester A. I., Keane A. J.; 2009. Recent advances in surrogate-based optimization. *Progress in Aerospace Sciences*, Vol 45, Issue 3, pp 50-79.

[6] Sandeep S., and Larsgunnar.; 2015. Multiobjective reliability-based and robust design optimisation for crashworthiness of a vehicle side impact. *International Journal of Vehicle Design*, Vol. 67, Issue 4, pp 215-225.
[7] Ryberg A.B., Backryd R.D., Nilsson L.; 2015. A metamodel-based multidisciplinary design optimization process for automotive structures. *Engineering with Computers Journal*, Vol 31, Issue 4, pp 711-728.
[8] Aalae B., Abderrahmane H., Gael M.; 2016. Computational design of an automotive twist beam. *Journal of Computational Design and Engineering*, Vol 3, Issue 3, pp 215-225.
[9] Su R., Gui L., Fan Z.; 2011. Multi-objective optimization for bus body with strength and rollover safety constraints based on surrogate models. *Structural and Multidisciplinary Optimization*, Vol 44, Issue 3, pp 431-441.
[10] Shinkyu J., Shigeru O., Kazuomi Y.; 2005. Aerodynamic Optimization Design with Kriging Model. *TRANSACTIONS OF THE JAPAN SOCIETY FOR AERONAUTICAL AND SPACE SCIENCES* , Vol 48, Issue 161, pp 161-168.
[11] Jouhaud J.-C., Sagaut P., Montagnac M., Laurenceau J.; 2007. A surrogate model based multi-disciplinary shape optimization method with application to a 2d subsonic airfoil. *Computers and Fluids*, Vol 36, Issue 3, pp 520-529.
[12] Jeong S., Murayama M., Yamamoto K.; 2005. Efficient optimization design method using kriging model. *Journal of Aircraft*, Vol 42, Issue 2, pp 413-419.
[13] Bryan E., Zheng O., Satish N., Vladimir A.F. and Igor M.; 2012. A methodology for meta-model based optimization in building energy models. *Energy and Buildings Journal*, Vol 47, pp 292-301.
[14] Messac A., Ismail-Yahaya A., Mattson C.A.; 2003. The normalized normal constraint method for generating the Pareto frontier. *Structural and Multidisciplinary Optimization*, Vol 25, Issue 2, pp 86-98.
[15] Messac A. , Mattson C.; 2004. Normal constraint method with guarantee of even representation of complete Pareto frontier. *AIAA Journal*, Vol 42, Issue 10, pp 2101-2111.
[16] Messac A. , Mattson C.; 2002. Generating well-distributed sets of Pareto points for engineering design using physical programming. *Optimization and Engineering*, Vol 3, Issue 10, pp 431-450.
[17] Powell M.J.D; 1992. The Theory of Radial Basis Function Approximation. *Advances in Numerical Analysis*, Vol 2, pp 105-210.
[18] Rippa S.; 2001. A Radial Basis Function Method for Global Optimization. *Journal of Global Optimization*, Vol 19, Issue 3, pp 201-227.
[19] Dyn N., Levin D., Rippa S.; 1986. Numerical Procedures for Surface Fitting of Scattered Data by Radial Basis Functions. *SIAM Journal of Scientific and Statistical Computing*, Vol 7, Issue 2, pp 639-659.
[20] Schaback R.; 1993. Comparison of radial basis function interpolants. *Journal*, in: K. Jetter and F. Utreras (eds), Multivariate Approximations: From CAGD to Wavelets, World Scientific, Singapore, 293-305.
[21] Duvigneau R., Chandrashekarappa P.; 2007. Radial Basis Functions and Kriging Metamodels for Aerodynamic Optimization. *INRIA report*, Id: inria-00137602, pp 9-13.
[22] Aalae B.; 2014. Methodes efficaces de capture de front de pareto en conception mecanique multicritere : applications industrielles *Nice University - Thesis*, pp 33-42.
[23] Rippa S.; 1999. An algorithm for selecting a good value for the parameter c in radial basis function interpolation. *Advances in Computational Mathematics Journal*, Vol 11, Issue 2, pp 193-210.